

LONG TIME STABILITY OF A LINEARLY EXTRAPOLATED BLENDED BDF SCHEME FOR MULTIPHYSICS FLOWS

AYTEKIN ÇIBIK, FATMA G. EROGLU, AND SONGUL KAYA*

Abstract. This paper investigates the long time stability behavior of multiphysics flow problems, namely the Navier-Stokes equations, natural convection and double-diffusive convection equations with an extrapolated blended BDF time-stepping scheme. This scheme combines the two-step BDF and three-step BDF time stepping schemes. We prove unconditional long time stability theorems for each of these flow systems. Various numerical tests are given for large time step sizes in long time intervals in order to support theoretical results.

Key words. Blended BDF, long time stability, Navier-Stokes, natural convection, double-diffusive.

1. Introduction

Most of the engineering and applied science problem involves the combination of some different physical problems such as fluid flow, heat transfer, mass transfer, and electromagnetic effect. These kinds of problems are mostly referred as multiphysics problems. From a mathematical point of view, these problems yield systems of coupled single physics equations. In our case, many important applications require the accurate solution of multiphysics coupling with Navier-Stokes equations. Since the simulation of Navier-Stokes equations has its own difficulties, the coupling among involved equations yield more complex problems. One possibility of improving numerical simulations is to develop algorithms which are reliable and robust. In addition, designed numerical schemes should capture the long time dynamics of the system in a right way. Thus, it is of practical interest to have an algorithm which is stable over the required long time intervals.

In recent years, considerable amount of effort has been spent to understand the long time behavior of the numerical schemes for multiphysics problems. For such works, we refer to [3, 6, 19, 20, 22, 24]. In particular, for Navier-Stokes equations, the Crank-Nicholson in [11, 12, 19], the implicit Euler in [22], two-step Backward Differentiation (BDF2) in [2] and fractional step/projection methods in [18] are chosen as temporal discretization in order to show the long time stability. In this respect, an extrapolated two step BDF scheme for a velocity-vorticity form of Navier-Stokes equations has been investigated in [10]. The long time stability of partitioned methods for the fully evolutionary Stokes-Darcy problem in [13], for the time dependent MHD system in [14, 20] and for the double-diffusive convection in [21] were also established based on implicit-explicit and backward differentiation schemes.

This study concerns the behavior of the solutions of multiphysics problems for longer time simulations and time step restrictions on these solutions. In order to solve the systems numerically, a finite element in space discretization is employed along with a rather new time stepping approach so called an extrapolated

Received by the editors March 11, 2016, and in revised form, March 17, 2019.

2000 *Mathematics Subject Classification.* 65M12, 65M60, 65N30.

*Corresponding Author.

blended Backward Differentiation (BLEBDF) temporal discretization. Such kind of a scheme combines BDF2 and a three-step BDF method in order to not only preserve A -stability and second order accuracy but also have a smaller constant in truncation error terms, [23]. Along with the mentioned time-stepping strategy, the three-step extrapolation is used in order to linearize the convective terms in the system of PDE's. Thus, the solution of only one linear system of equations is encountered at each time step which reduces the compilation time and memory cost in simulations.

In [17], Ravindran considers the stability and convergence of a double diffusive convection system with the blended BDF scheme in short time intervals. The current study attempts to extend the works above to study the notion of long time stability by combining the BLEBDF idea and its effects on several multiphysics flows such as Navier-Stokes, natural convection and double-diffusive convection. In this work, we will provide the unconditional long time L^2 stability property of BLEBDF method for each of flow systems, when they are discretized spatially with finite element method. To the best of authors' knowledge, this is the first study that investigates the long time stability of the finite element solutions of multiphysics flows involving a blended BDF time-stepping approach along with a third order linear extrapolation idea.

The plan of the paper is as follows. In Section 2, we state the notations with some mathematical preliminaries. Section 3 is reserved for proving the unconditional long time stability of Navier-Stokes equations under the employment of extrapolated blended BDF temporal discretization along with numerical experiments. Similar results are established for natural convection and double-diffusive convection equations in Section 4 and Section 5, respectively. Finally, we state some conclusion remarks in the last section.

2. Notations and Preliminaries

Let $\Omega \subset \mathbb{R}^d$, $d \in \{2, 3\}$, be open, connected domain bounded by Lipschitz boundary $\partial\Omega$. Throughout the paper standard notations for Sobolev spaces and their norms will be used, c.f. Adams [1]. The norm in $(H^k(\Omega))^d$ is denoted by $\|\cdot\|_k$ and the norm in Lebesgue spaces $(L^p(\Omega))^d$, $1 \leq p < \infty$, $p \neq 2$ by $\|\cdot\|_{L^p}$ and $p = \infty$ by $\|\cdot\|_\infty$. The space $L^2(\Omega)$ is equipped with the norm and inner product $\|\cdot\|$ and (\cdot, \cdot) , respectively, and for these we drop the subscripts. Vector-valued functions will be identified by bold face. The norm in dual space H^{-1} of $H_0^1(\Omega)$ is denoted by $\|\cdot\|_{-1}$. The continuous velocity, pressure, temperature and concentration spaces are denoted by

$$\mathbf{X} := (\mathbf{H}_0^1(\Omega))^d, \quad Q := L_0^2(\Omega), \quad W := H_0^1(\Omega), \quad \Psi := H_0^1(\Omega),$$

and the divergence free space

$$\mathbf{V} = \{\mathbf{v} \in \mathbf{X} : (\nabla \cdot \mathbf{v}, q) = 0, \forall q \in Q\}.$$

We recall also the Poincaré-Friedrichs inequality as

$$\|\mathbf{v}\| \leq C_P \|\nabla \mathbf{v}\|, \quad \forall \mathbf{v} \in \mathbf{X}.$$

For each multiphysics flow problems, we consider a regular, conforming family Π^h of triangulations of domain with maximum diameter h for spatial discretization. Assume $\mathbf{X}_h \subset \mathbf{X}$, $Q_h \subset Q$, $W_h \subset W$ and $\Psi_h \subset \Psi$ be finite element spaces such that the spaces (\mathbf{X}_h, Q_h) satisfy the discrete inf-sup condition needed for stability of the discrete pressure, [5]. The discretely divergence free space for (\mathbf{X}_h, Q_h) pair

is given by

$$(1) \quad \mathbf{V}_h = \{\mathbf{v}_h \in \mathbf{X}_h : (\nabla \cdot \mathbf{v}_h, q_h) = 0, \forall q_h \in Q_h\}.$$

The dual spaces of \mathbf{V}_h , W_h and Ψ_h are given by \mathbf{V}_h^* , W_h^* and Ψ_h^* , and their norms are denoted by $\|\cdot\|_{\mathbf{V}_h^*}$, $\|\cdot\|_{W_h^*}$ and $\|\cdot\|_{\Psi_h^*}$ respectively. We also need the following space in the analysis

$$(2) \quad L^\infty(\mathbb{R}_+, \mathbf{V}_h^*) := \{\mathbf{f} : \Omega^d \times \mathbb{R}_+ \rightarrow \mathbb{R}^d, \exists K < \infty, a.e. t > 0, \|\mathbf{f}(t)\|_{\mathbf{V}_h^*} < K\}.$$

Similar spaces for W_h^* and Ψ_h^* will be used throughout the analysis. To simplify the analysis, we utilize the G -stability framework as in [8]. For third order backward differentiation, the positive definite matrix G -matrix and the associated norm can be obtained as

$$G = \frac{1}{12} \begin{pmatrix} 19 & -12 & 3 \\ -12 & 10 & -3 \\ 3 & -3 & 1 \end{pmatrix}, \quad \|\mathcal{W}\|_G^2 = (\mathcal{W}, G\mathcal{W}). \quad \mathcal{W} \in \mathbb{R}^{3n}.$$

The following relations are well-known and required for the analysis.

Lemma 2.1. *G -norm and L^2 norm are equivalent in the sense that there exist $0 < C_l < C_u$ positive constants such that*

$$(3) \quad C_l \|\mathcal{W}\|_G^2 \leq \|\mathcal{W}\|^2 \leq C_u \|\mathcal{W}\|_G^2.$$

Proof. See reference [8]. □

Lemma 2.2. *The following estimates hold:*

$$(4) \quad \left\| \begin{bmatrix} \mathbf{u} \\ \mathbf{v} \\ \mathbf{w} \end{bmatrix} \right\|_G^2 \geq \frac{1}{3} \|\mathbf{u}\|^2 - \frac{5}{12} \|\mathbf{v}\|^2 - \frac{5}{12} \|\mathbf{w}\|^2,$$

$$(5) \quad \left\| \begin{bmatrix} \mathbf{u} \\ \mathbf{v} \\ \mathbf{w} \end{bmatrix} \right\|_G^2 \leq \frac{19}{12} \|\mathbf{u}\|^2 + \frac{10}{12} \|\mathbf{v}\|^2 + \frac{1}{12} \|\mathbf{w}\|^2.$$

Proof. Using the properties of inner product and norm, we have

$$(6) \quad \left\| \begin{bmatrix} \mathbf{u} \\ \mathbf{v} \\ \mathbf{w} \end{bmatrix} \right\|_G^2 = \left(\begin{bmatrix} \mathbf{u} \\ \mathbf{v} \\ \mathbf{w} \end{bmatrix}, G \begin{bmatrix} \mathbf{u} \\ \mathbf{v} \\ \mathbf{w} \end{bmatrix} \right) = \frac{1}{3} \|\mathbf{u}\|^2 - \frac{5}{12} \|\mathbf{v}\|^2 - \frac{5}{12} \|\mathbf{w}\|^2 + \|\mathbf{u} - \mathbf{v}\|^2 + \frac{3}{12} \|\mathbf{u} + \mathbf{w}\|^2 + \frac{3}{12} \|\mathbf{v} - \mathbf{w}\|^2.$$

Dropping last three non-negative terms yields (4). In a similar manner, deleting non-positive terms in (6) and using the triangle inequality gives (5). □

Lemma 2.3. *The symmetric matrix $G \in \mathbb{R}^{3n \times 3n}$ which is given above satisfies the following equality $\forall \{\mathbf{w}_h^j\}_{j=0}^N \subset L^2(\Omega)$:*

$$(7) \quad \begin{aligned} & \left(\frac{5}{3} \mathbf{w}_h^{n+1} - \frac{5}{2} \mathbf{w}_h^n + \mathbf{w}_h^{n-1} - \frac{1}{6} \mathbf{w}_h^{n-2}, \mathbf{w}_h^{n+1} \right) \\ & = \|\mathcal{W}_{n+1}\|_G^2 - \|\mathcal{W}_n\|_G^2 + \frac{1}{12} \|\mathbf{w}_h^{n+1} - 3\mathbf{w}_h^n + 3\mathbf{w}_h^{n-1} - \mathbf{w}_h^{n-2}\|^2, \end{aligned}$$

where $\mathcal{W}_{n+1} = [\mathbf{w}_h^{n+1} \quad \mathbf{w}_h^n \quad \mathbf{w}_h^{n-1}]^\top$ and $\mathcal{W}_n = [\mathbf{w}_h^n \quad \mathbf{w}_h^{n-1} \quad \mathbf{w}_h^{n-2}]^\top$.

Proof. To prove this, we use a well-known identity (see [17]) to obtain

$$\begin{aligned}
& \left(\frac{5}{3} \mathbf{w}_h^{n+1} - \frac{5}{2} \mathbf{w}_h^n + \mathbf{w}_h^{n-1} - \frac{1}{6} \mathbf{w}_h^{n-2}, \mathbf{w}_h^{n+1} \right) \\
&= \left(\|\mathbf{w}_h^{n+1}\|^2 + \|3\mathbf{w}_h^{n+1} - \mathbf{w}_h^n\|^2 + \|3\mathbf{w}_h^{n+1} - 3\mathbf{w}_h^n + \mathbf{w}_h^{n-1}\|^2 \right) \\
&\quad - \left(\|\mathbf{w}_h^n\|^2 + \|3\mathbf{w}_h^n - \mathbf{w}_h^{n-1}\|^2 + \|3\mathbf{w}_h^n - 3\mathbf{w}_h^{n-1} + \mathbf{w}_h^{n-2}\|^2 \right) \\
(8) \quad &+ \frac{1}{12} \|\mathbf{w}_h^{n+1} - 3\mathbf{w}_h^n + 3\mathbf{w}_h^{n-1} - \mathbf{w}_h^{n-2}\|^2.
\end{aligned}$$

Using the properties of G -norm and inner product, one gets

$$\begin{aligned}
& \|\mathbf{w}_h^{n+1}\|^2 + \|3\mathbf{w}_h^{n+1} - \mathbf{w}_h^n\|^2 + \|3\mathbf{w}_h^{n+1} - 3\mathbf{w}_h^n + \mathbf{w}_h^{n-1}\|^2 \\
(9) \quad &= \left(\begin{bmatrix} \mathbf{w}_h^{n+1} \\ \mathbf{w}_h^n \\ \mathbf{w}_h^{n-1} \end{bmatrix}, G \begin{bmatrix} \mathbf{w}_h^{n+1} \\ \mathbf{w}_h^n \\ \mathbf{w}_h^{n-1} \end{bmatrix} \right) = \left\| \begin{bmatrix} \mathbf{w}_h^{n+1} \\ \mathbf{w}_h^n \\ \mathbf{w}_h^{n-1} \end{bmatrix} \right\|_G^2 = \|\mathcal{W}_{n+1}\|_G^2.
\end{aligned}$$

Obtaining $\|\mathcal{W}_n\|_G^2$ similar with (9) and inserting them in (8) yields (7). \square

3. Long time stability of Navier-Stokes equations with BLEBDF

The goal of this section is to show that our scheme is unconditionally long-time stable. That is, the solutions remain bounded without any time step restriction. We first study an extrapolated blended BDF method for discretizing the incompressible NSE:

$$\begin{aligned}
(10) \quad & \mathbf{u}_t - \nu \Delta \mathbf{u} + (\mathbf{u} \cdot \nabla) \mathbf{u} + \nabla p = \mathbf{f} \quad \text{in } \Omega, \\
& \nabla \cdot \mathbf{u} = 0 \quad \text{in } \Omega, \\
& \mathbf{u} = \mathbf{0} \quad \text{on } \partial\Omega, \\
& \mathbf{u}(0, \mathbf{x}) = \mathbf{u}_0 \quad \text{in } \Omega, \\
& \int_{\Omega} p \, d\mathbf{x} = 0.
\end{aligned}$$

where \mathbf{u} is the velocity field, p is the fluid pressure, ν is the kinematic viscosity and \mathbf{f} denotes the body force. The variational formulation of (10) reads as follows: Find $(\mathbf{u}, p) \in (\mathbf{X}, Q)$ satisfying

$$\begin{aligned}
(11) \quad & (\mathbf{u}_t, \mathbf{v}) + \nu(\nabla \mathbf{u}, \nabla \mathbf{v}) + b_1(\mathbf{u}, \mathbf{u}, \mathbf{v}) - (p, \nabla \cdot \mathbf{v}) = (\mathbf{f}, \mathbf{v}) \quad \forall \mathbf{v} \in \mathbf{X}, \\
& (\nabla \cdot \mathbf{u}, q) = 0 \quad \forall q \in Q,
\end{aligned}$$

where

$$(12) \quad b_1(\mathbf{u}, \mathbf{v}, \mathbf{w}) := \frac{1}{2} (((\mathbf{u} \cdot \nabla) \mathbf{v}, \mathbf{w}) - ((\mathbf{u} \cdot \nabla) \mathbf{w}, \mathbf{v})),$$

represents the skew-symmetric form of the convective term. Note that the convective term has the well known property

$$(13) \quad b_1(\mathbf{u}, \mathbf{v}, \mathbf{v}) = 0$$

for all $\mathbf{u}, \mathbf{v} \in \mathbf{X}$, which simplifies the analysis.

The studied time discretization method uses different time discretizations for different terms. The scheme discretizes in time via a BDF2 and a BDF3 scheme whereas the nonlinear terms are treated via a third-order extrapolation formula. One consequence of lagging the nonlinear term to previous time levels is to avoid solving nonlinear equations. A class of this type of blending BDF schemes which are also known as a class of optimized second-order BDF schemes are proposed in

[15, 23]. We now consider one of the special case of this family proposed in [23], with an error constant half as large as BDF2 scheme.

Based on the weak formulation (10), the fully discrete approximation of it reads as follows. Given \mathbf{f} , $\mathbf{u}_h^0 = \mathbf{u}_h^{-1} = \mathbf{u}_h^{-2} = \mathbf{u}_0$, for any time step $\Delta t > 0$, find $(\mathbf{u}_h^{n+1}, p_h^{n+1}) \in (\mathbf{X}_h, Q_h)$ such that for $n \geq 0$

$$(14) \quad \left(\frac{\frac{5}{3}\mathbf{u}_h^{n+1} - \frac{5}{2}\mathbf{u}_h^n + \mathbf{u}_h^{n-1} - \frac{1}{6}\mathbf{u}_h^{n-2}}{\Delta t}, \mathbf{v}_h \right) + \nu(\nabla \mathbf{u}_h^{n+1}, \nabla \mathbf{v}_h) \\ + b_1(3\mathbf{u}_h^n - 3\mathbf{u}_h^{n-1} + \mathbf{u}_h^{n-2}, \mathbf{u}_h^{n+1}, \mathbf{v}_h) - (p_h^{n+1}, \nabla \cdot \mathbf{v}_h) = (\mathbf{f}^{n+1}, \mathbf{v}_h),$$

$$(15) \quad (\nabla \cdot \mathbf{u}_h^{n+1}, q_h) = 0$$

for all $(\mathbf{v}_h, q_h) \in (\mathbf{X}_h, Q_h)$.

We now analyze the long time stability over $0 \leq t^n < \infty$ and show that the scheme is uniformly bounded in time in L^2 norm. Our proof is based on a G -norm and the associated estimation (7).

Theorem 3.1. (Unconditional long time stability of NSE in L^2) Assume $\mathbf{f} \in L^\infty(\mathbb{R}_+, \mathbf{V}_h^*)$, then the approximation (14)-(15) is long time stable in the following sense: for any $\Delta t > 0$,

$$(16) \quad \|\mathcal{U}_{n+1}\|_G^2 + \frac{\nu\Delta t}{4}\|\nabla \mathbf{u}_h^{n+1}\|^2 + \frac{\nu\Delta t}{16}\|\nabla \mathbf{u}_h^n\|^2 \leq (1 + \alpha)^{-(n+1)}(\|\mathcal{U}_0\|_G^2 \\ + \frac{\nu\Delta t}{4}\|\nabla \mathbf{u}_h^0\|^2 + \frac{\nu\Delta t}{16}\|\nabla \mathbf{u}_h^{-1}\|^2) + \max\left\{\frac{8C_p^2}{C_l\nu^2}, \frac{2\nu^{-1}\Delta t}{3}\right\}\|\mathbf{f}\|_{L^\infty(\mathbb{R}_+; \mathbf{V}_h^*)}^2.$$

where $\mathcal{U}_0 = [\mathbf{u}_h^0 \quad \mathbf{u}_h^{-1} \quad \mathbf{u}_h^{-2}]$ and $\alpha = \min\left\{\frac{C_l\nu\Delta t}{16C_p^2}, \frac{3}{4}\right\}$.

Remark 3.1. Theorem implies that the result holds for any large n , since the constants are independent of n .

Proof. Setting $\mathbf{v}_h = \mathbf{u}_h^{n+1}$ in (14) and $q_h = p_h^{n+1}$ in (15) the BLEBDF scheme and using the skew-symmetry property (13), we obtain

$$(17) \quad \left(\frac{\frac{5}{3}\mathbf{u}_h^{n+1} - \frac{5}{2}\mathbf{u}_h^n + \mathbf{u}_h^{n-1} - \frac{1}{6}\mathbf{u}_h^{n-2}}{\Delta t}, \mathbf{u}_h^{n+1} \right) + \nu(\nabla \mathbf{u}_h^{n+1}, \nabla \mathbf{u}_h^{n+1}) \\ = (\mathbf{f}^{n+1}, \mathbf{u}_h^{n+1}).$$

From (7), we get

$$(18) \quad \|\mathcal{U}_{n+1}\|_G^2 - \|\mathcal{U}_n\|_G^2 + \frac{1}{12}\|\mathbf{u}_h^{n+1} - 3\mathbf{u}_h^n + 3\mathbf{u}_h^{n-1} - \mathbf{u}_h^{n-2}\|^2 + \nu\Delta t\|\nabla \mathbf{u}_h^{n+1}\|^2 \\ = \Delta t(\mathbf{f}^{n+1}, \mathbf{u}_h^{n+1}).$$

where $\mathcal{U}_{n+1} = [\mathbf{u}_h^{n+1} \quad \mathbf{u}_h^n \quad \mathbf{u}_h^{n-1}]^\top$ and $\mathcal{U}_n = [\mathbf{u}_h^n \quad \mathbf{u}_h^{n-1} \quad \mathbf{u}_h^{n-2}]^\top$. Applying the Cauchy-Schwarz and Young's inequalities for the right hand side of (18) gives

$$(19) \quad \|\mathcal{U}_{n+1}\|_G^2 - \|\mathcal{U}_n\|_G^2 + \frac{1}{12}\|\mathbf{u}_h^{n+1} - 3\mathbf{u}_h^n + 3\mathbf{u}_h^{n-1} - \mathbf{u}_h^{n-2}\|^2 + \frac{\nu\Delta t}{2}\|\nabla \mathbf{u}_h^{n+1}\|^2 \\ \leq \frac{\nu^{-1}\Delta t}{2}\|\mathbf{f}^{n+1}\|_{\mathbf{V}_h^*}^2.$$

Adding $\frac{\nu\Delta t}{4}\|\nabla\mathbf{u}_h^n\|^2 + \frac{\nu\Delta t}{16}\|\nabla\mathbf{u}_h^{n-1}\|^2$ to the both sides and discarding the third positive term in the left hand side of (19) yield

$$(20) \quad \left(\|\mathcal{U}_{n+1}\|_G^2 + \frac{\nu\Delta t}{4}\|\nabla\mathbf{u}_h^{n+1}\|^2 + \frac{\nu\Delta t}{16}\|\nabla\mathbf{u}_h^n\|^2 \right) + \frac{\nu\Delta t}{16}\left(\|\nabla\mathbf{u}_h^{n+1}\|^2 + \|\nabla\mathbf{u}_h^n\|^2 + \|\nabla\mathbf{u}_h^{n-1}\|^2 \right) + \frac{3\nu\Delta t}{16}\|\nabla\mathbf{u}_h^{n+1}\|^2 + \frac{\nu\Delta t}{8}\|\nabla\mathbf{u}_h^n\|^2 \\ \leq \|\mathcal{U}_n\|_G^2 + \frac{\nu\Delta t}{4}\|\nabla\mathbf{u}_h^n\|^2 + \frac{\nu\Delta t}{16}\|\nabla\mathbf{u}_h^{n-1}\|^2 + \frac{\nu^{-1}\Delta t}{2}\|\mathbf{f}^{n+1}\|_{\mathbf{V}_h^*}^2.$$

The terms in the left hand side of (20) can be rearranged by applying the Poincaré-Friedrichs and the equivalent norm property (3):

$$(21) \quad \frac{\nu\Delta t}{16}\left(\|\nabla\mathbf{u}_h^{n+1}\|^2 + \|\nabla\mathbf{u}_h^n\|^2 + \|\nabla\mathbf{u}_h^{n-1}\|^2 \right) + \frac{3\nu\Delta t}{16}\|\nabla\mathbf{u}_h^{n+1}\|^2 \\ + \frac{\nu\Delta t}{8}\|\nabla\mathbf{u}_h^n\|^2 \\ \geq \frac{C_l\nu\Delta t}{16C_p^2}\|\mathcal{U}_{n+1}\|_G^2 + \frac{3\nu\Delta t}{16}\|\nabla\mathbf{u}_h^{n+1}\|^2 + \frac{\nu\Delta t}{8}\|\nabla\mathbf{u}_h^n\|^2 \\ \geq \alpha\left(\|\mathcal{U}_{n+1}\|_G^2 + \frac{\nu\Delta t}{4}\|\nabla\mathbf{u}_h^{n+1}\|^2 + \frac{\nu\Delta t}{16}\|\nabla\mathbf{u}_h^n\|^2 \right),$$

where $\alpha = \min\left\{\frac{C_l\nu\Delta t}{16C_p^2}, \frac{3}{4}\right\}$. Inserting (21) in (20) and using induction along with $\|\mathbf{f}^i\|_{\mathbf{V}_h^*}^2 \leq \|\mathbf{f}\|_{L^\infty(\mathbb{R}_+; \mathbf{V}_h^*)}^2, \forall i = 1, \dots, n+1$ gives

$$(22) \quad \left(\|\mathcal{U}_{n+1}\|_G^2 + \frac{\nu\Delta t}{4}\|\nabla\mathbf{u}_h^{n+1}\|^2 + \frac{\nu\Delta t}{16}\|\nabla\mathbf{u}_h^n\|^2 \right) \\ \leq (1+\alpha)^{-(n+1)}\left(\|\mathcal{U}_0\|_G^2 + \frac{\nu\Delta t}{4}\|\nabla\mathbf{u}_h^0\|^2 + \frac{\nu\Delta t}{16}\|\nabla\mathbf{u}_h^{-1}\|^2 \right) \\ + \frac{(1+\alpha)^{-1}\nu^{-1}\Delta t}{2}\|\mathbf{f}\|_{L^\infty(\mathbb{R}_+; \mathbf{V}_h^*)}^2 \left((1+\alpha)^{-n} \right. \\ \left. + (1+\alpha)^{-(n-1)} + \dots + 1 \right).$$

Since $|\frac{1}{1+\alpha}| < 1$, then we get

$$(23) \quad \left(\|\mathcal{U}_{n+1}\|_G^2 + \frac{\nu\Delta t}{4}\|\nabla\mathbf{u}_h^{n+1}\|^2 + \frac{\nu\Delta t}{16}\|\nabla\mathbf{u}_h^n\|^2 \right) \\ \leq (1+\alpha)^{-(n+1)}\left(\|\mathcal{U}_0\|_G^2 + \frac{\nu\Delta t}{4}\|\nabla\mathbf{u}_h^0\|^2 + \frac{\nu\Delta t}{16}\|\nabla\mathbf{u}_h^{-1}\|^2 \right) \\ + \max\left\{ \frac{8C_p^2}{C_l\nu^2}, \frac{2\nu^{-1}\Delta t}{3} \right\} \|\mathbf{f}\|_{L^\infty(\mathbb{R}_+; \mathbf{V}_h^*)}^2$$

which is the required result. \square

3.1. Numerical experiment for Navier-Stokes equations. Throughout this paper, we carry out tests for each flow problem separately. We expose the evolution of the L^2 norm of solution variables in long time intervals for each variable according to related problems. After each numerical test, we provide a table showing the CPU-times of relevant simulations according to varying Δt and compare these CPU-times with classical BDF2 methods' CPU-times in order to reveal the computational advantage of the method. We choose the inf-sup stable Scott-Vogelius

finite element pair for velocity-pressure couple, which is known to be discretely divergence free. We refer [4], for the details of this selection. Throughout all our simulations, we use public license finite element software package FreeFem++, [9].

We now perform a numerical test in order to verify theoretical long time stability result obtained in Theorem 3.1. We set $\Omega = (0, 1)^2$ with a coarse mesh resolution of 16×16 . We calculate the approximate solution in time interval $[0, 400]$ and calculate the L^2 norms for different Δt and varying ν . We pick the initial velocity and the forcing term for this test problem as :

$$(24) \quad \mathbf{u} = \begin{pmatrix} \sin(\pi x) \sin(\pi y) \\ \cos(\pi x) \cos(\pi y) \end{pmatrix}, \quad f = \begin{pmatrix} y^2 \cos(xy^2) + \sin(x) \sin(y) \\ 2xy \cos(xy^2) + \cos(x) \cos(y) \end{pmatrix}.$$

In Figure 1, we present the evolution of $\|\mathbf{u}^{n+1}\|$ in long time interval $[0, 400]$. We give the stability results for two large time step instances for each case. As could be easily deduced from the figure, the solutions we obtain from the proposed scheme are long time stable even by using large time step sizes. Although slight deviations seem to occur due to small viscosity for the case $\nu = 0.001$, still the solution is within an interval of stability. Notice that, these solutions are obtained for a very coarse mesh resolution of 16×16 . Hence, small oscillations inside a narrow interval does not degrade the stability of the solution.

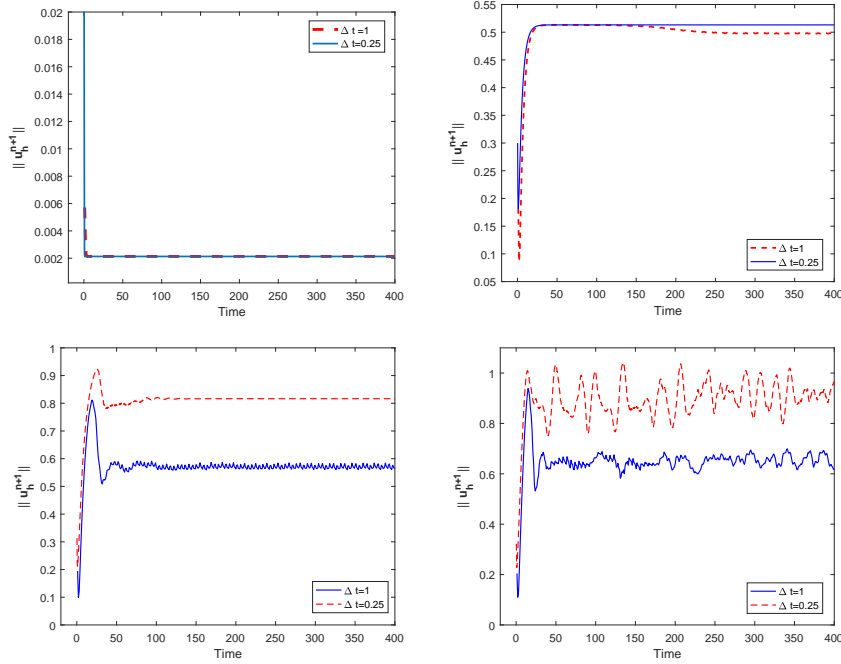


FIGURE 1. Evolution of the L^2 norm of the velocity solution for varying ν . $\nu = 1$, $\nu = 0.004$ (upper left to right) and $\nu = 0.002$, $\nu = 0.001$ (lower left to right).

We also compare the CPU times of the scheme (14)-(15) and run the same problem in a shorter time interval $[0, 150]$. As could be observed from Table 1, the BLEBDF scheme has an advantage in terms of simulation CPU times when compared with a classical BDF2 scheme. When Δt becomes smaller, the difference

between the CPU times are increasing. This shows the promise of the method, especially when smaller time step sizes are used.

TABLE 1. Comparison of the CPU-times (seconds) of classical BDF2 scheme and BLEBDF for the Navier-Stokes equations with $\nu = 0.001$ on a time interval $[0, 150]$.

Δt	BDF2	BLEBDF
1	1.37	0.87
0.1	12	8
0.01	131.5	78.7

4. Long time stability of natural convection equations with BLEBDF

In this section, we prove that the BLEBDF scheme for natural convection equations is also long time stable. The unsteady natural convection system in Ω with partitioned boundary $\partial\Omega = \Gamma_T \cup \Gamma_B$ with $\Gamma_T \cap \Gamma_B = \emptyset$, the so called Boussinesq equations are given by

$$\begin{aligned}
(25) \quad & \mathbf{u}_t - \nu \Delta \mathbf{u} + (\mathbf{u} \cdot \nabla) \mathbf{u} + \nabla p = Ri T \mathbf{e}_2 + \mathbf{f} && \text{in } \Omega, \\
& \nabla \cdot \mathbf{u} = 0 && \text{in } \Omega, \\
& T_t - \nabla \cdot (\kappa \nabla T) + (\mathbf{u} \cdot \nabla) T = \gamma && \text{in } \Omega, \\
& \mathbf{u}(0, \mathbf{x}) = \mathbf{u}_0, T(0, \mathbf{x}) = T_0 && \text{in } \Omega, \\
& \mathbf{u} = \mathbf{0} \text{ on } \partial\Omega, T = 0 \text{ on } \Gamma_T, \frac{\partial T}{\partial \mathbf{n}} = 0 && \text{on } \Gamma_B,
\end{aligned}$$

where \mathbf{u} , p , T are the fluid velocity, the pressure and the temperature, respectively. The parameters in (25) are the kinematic viscosity ν , the thermal conductivity parameter $\kappa > 0$ and the Richardson number Ri and the unit vector is given by \mathbf{e}_2 . The prescribed body forces are \mathbf{f} and γ . The initial velocity and temperature are \mathbf{u}_0 and T_0 , respectively.

By using similar notations as in Section 3, given \mathbf{f} , γ , $\mathbf{u}_h^0 = \mathbf{u}_h^{-1} = \mathbf{u}_h^{-2} = \mathbf{u}_0$ and $T_h^0 = T_h^{-1} = T_h^{-2} = T_0$ find $(\mathbf{u}_h^{n+1}, p_h^{n+1}, T_h^{n+1}) \in (\mathbf{X}_h, Q_h, W_h)$ for $n \geq 1$ satisfying

$$\begin{aligned}
(26) \quad & \left(\frac{\frac{5}{3} \mathbf{u}_h^{n+1} - \frac{5}{2} \mathbf{u}_h^n + \mathbf{u}_h^{n-1} - \frac{1}{6} \mathbf{u}_h^{n-2}}{\Delta t}, \mathbf{v}_h \right) + \nu (\nabla \mathbf{u}_h^{n+1}, \nabla \mathbf{v}_h) \\
& + b_1(\mathbf{u}^*, \mathbf{u}_h^{n+1}, \mathbf{v}_h) - (p_h, \nabla \cdot \mathbf{u}_h^{n+1}) = Ri (T^* \mathbf{e}_2, \mathbf{v}_h) + (\mathbf{f}^{n+1}, \mathbf{v}_h),
\end{aligned}$$

$$(27) \quad (q_h, \nabla \cdot \mathbf{v}_h^{n+1}) = 0$$

$$\begin{aligned}
(28) \quad & \left(\frac{\frac{5}{3} T_h^{n+1} - \frac{5}{2} T_h^n + T_h^{n-1} - \frac{1}{6} T_h^{n-2}}{\Delta t}, S_h \right) + \kappa (\nabla T_h^{n+1}, \nabla S_h) \\
& + b_2(\mathbf{u}^*, T_h^{n+1}, S_h) = (\gamma^{n+1}, S_h),
\end{aligned}$$

for all $(\mathbf{v}_h, q_h, S_h) \in (\mathbf{X}_h, Q_h, W_h)$ where $\mathbf{u}^* = 3\mathbf{u}_h^n - 3\mathbf{u}_h^{n-1} + \mathbf{u}_h^{n-2}$ and $T^* = 3T_h^n - 3T_h^{n-1} + T_h^{n-2}$. Herein the related skew-symmetric form is given by

$$(29) \quad b_2(\mathbf{u}, T, S) := \frac{1}{2} (((\mathbf{u} \cdot \nabla) T, S) - ((\mathbf{u} \cdot \nabla) S, T))$$

for all $\mathbf{u} \in \mathbf{X}, T, S \in W$.

Theorem 4.1. (Unconditional long time stability of natural convection in L^2) Assume $\mathbf{f} \in L^\infty(\mathbb{R}_+, \mathbf{V}_h^*)$ and $\gamma \in L^\infty(\mathbb{R}_+, W_h^*)$, then the approximation (26)-(28) is long time stable in the following sense: for any $\Delta t > 0$,

$$\begin{aligned}
& \|\mathcal{U}_{n+1}\|_G^2 + \|\mathcal{T}_{n+1}\|_G^2 + \frac{\nu\Delta t}{4}\|\nabla\mathbf{u}_h^{n+1}\|^2 + \frac{\kappa\Delta t}{4}\|\nabla T_h^{n+1}\|^2 \\
& \leq (1+\alpha)^{-(n+1)}\left(\|\mathcal{U}_0\|_G^2 + \frac{\nu\Delta t}{4}\|\nabla\mathbf{u}_h^0\|^2 + \frac{\nu\Delta t}{16}\|\nabla\mathbf{u}_h^{-1}\|^2\right) \\
& \quad + (K_\alpha + (1+\beta)^{-1})\left((1+\beta)^{-n}(\|\mathcal{T}_0\|_G^2 + \frac{\kappa\Delta t}{4}\|\nabla T_h^0\|^2 + \frac{\kappa\Delta t}{16}\|\nabla T_h^{-1}\|^2)\right) \\
& \quad + (K_\alpha + 1)\max\left\{\frac{8C_p^2}{C_l\kappa^2}, \frac{2\kappa^{-1}\Delta t}{3}\right\}\|\gamma\|_{L^\infty(\mathbb{R}_+, W_h^*)}^2 \\
(30) \quad & \quad + \max\left\{\frac{16C_p^2}{C_l\nu^2}, \frac{4\nu^{-1}\Delta t}{3}\right\}\|\mathbf{f}\|_{L^\infty(\mathbb{R}_+, \mathbf{V}_h^*)}
\end{aligned}$$

where $K_\alpha = \frac{49C_u C_p^2 \nu^{-1} Ri^2 \Delta t}{\alpha}$, $\mathcal{U}_0 = [\mathbf{u}_h^0 \quad \mathbf{u}_h^{-1} \quad \mathbf{u}_h^{-2}]$, $\mathcal{T}_0 = [T_h^0 \quad T_h^{-1} \quad T_h^{-2}]$,
 $\alpha = \min\left\{\frac{C_l\nu\Delta t}{16C_p^2}, \frac{3}{4}\right\}$, $\beta = \min\left\{\frac{C_l\kappa\Delta t}{16C_p^2}, \frac{3}{4}\right\}$,

Proof. The proof starts with a stability bound for temperature. Letting $S_h = T_h^{n+1}$ in (28) and using the skew symmetry property $b_2(\mathbf{u}^*, T_h^{n+1}, T_h^{n+1}) = 0$. Along with (7) and multiplying with Δt yields

$$\begin{aligned}
& \|\mathcal{T}_{n+1}\|_G^2 - \|\mathcal{T}_n\|_G^2 + \frac{1}{12}\|T_h^{n+1} - 3T_h^n + 3T_h^{n-1} - T_h^{n-2}\|^2 + \kappa\Delta t\|\nabla T_h^{n+1}\|^2 \\
(31) \quad & \quad = \Delta t(\gamma^{n+1}, T_h^{n+1}).
\end{aligned}$$

where $\mathcal{T}_{n+1} = [T_h^{n+1} \quad T_h^n \quad T_h^{n-1}]^\top$ and $\mathcal{T}_n = [T_h^n \quad T_h^{n-1} \quad T_h^{n-2}]^\top$. Applying the Cauchy-Schwarz and Young's inequalities lead to

$$\begin{aligned}
& \|\mathcal{T}_{n+1}\|_G^2 - \|\mathcal{T}_n\|_G^2 + \frac{1}{12}\|T_h^{n+1} - 3T_h^n + 3T_h^{n-1} - T_h^{n-2}\|^2 + \frac{\kappa\Delta t}{2}\|\nabla T_h^{n+1}\|^2 \\
(32) \quad & \quad \leq \frac{\kappa^{-1}\Delta t}{2}\|\gamma^{n+1}\|_{W_h^*}^2.
\end{aligned}$$

Adding $\frac{\kappa\Delta t}{4}\|\nabla T_h^n\|^2 + \frac{\kappa\Delta t}{16}\|\nabla T_h^{n-1}\|^2$ to the both sides and dropping the nonnegative terms produce

$$\begin{aligned}
& (\|\mathcal{T}_{n+1}\|_G^2 + \frac{\kappa\Delta t}{4}\|\nabla T_h^{n+1}\|^2 + \frac{\kappa\Delta t}{16}\|\nabla T_h^n\|^2) + \frac{\kappa\Delta t}{16}(\|\nabla T_h^{n+1}\|^2 \\
& \quad + \|\nabla T_h^n\|^2 + \|\nabla T_h^{n-1}\|^2) + \frac{3\kappa\Delta t}{16}\|\nabla T_h^{n+1}\|^2 + \frac{\kappa\Delta t}{8}\|\nabla T_h^n\|^2 \\
(33) \quad & \leq \|\mathcal{T}_n\|_G^2 + \frac{\kappa\Delta t}{4}\|\nabla T_h^n\|^2 + \frac{\kappa\Delta t}{16}\|\nabla T_h^{n-1}\|^2 + \frac{\kappa^{-1}\Delta t}{2}\|\gamma^{n+1}\|_{W_h^*}^2.
\end{aligned}$$

The estimation of (33) follows closely that of (21). Again, the last five terms of the left hand side of (33) can be rearranged by the applying the Poincaré-Friedrichs and the equivalent norm property (3) as

$$\begin{aligned}
& \frac{\kappa\Delta t}{16}(\|\nabla T_h^{n+1}\|^2 + \|\nabla T_h^n\|^2 + \|\nabla T_h^{n-1}\|^2) \\
& \quad + \frac{3\kappa\Delta t}{16}\|\nabla T_h^{n+1}\|^2 + \frac{\kappa\Delta t}{8}\|\nabla T_h^n\|^2 \\
(34) \quad & \geq \beta(\|\mathcal{T}_{n+1}\|_G^2 + \frac{\kappa\Delta t}{4}\|\nabla T_h^{n+1}\|^2 + \frac{\kappa\Delta t}{16}\|\nabla T_h^n\|^2),
\end{aligned}$$

where $\beta = \min\{\frac{C_l \kappa \Delta t}{16C_p^2}, \frac{3}{4}\}$. Arguing as before and inserting (34) in (33) and using induction leads to

$$\begin{aligned}
& \|\mathcal{T}_{n+1}\|_G^2 + \frac{\kappa \Delta t}{4} \|\nabla T_h^{n+1}\|^2 + \frac{\kappa \Delta t}{16} \|\nabla T_h^n\|^2 \\
& \leq (1 + \beta)^{-(n+1)} (\|\mathcal{T}_0\|_G^2 + \frac{\kappa \Delta t}{4} \|\nabla T_h^0\|^2 + \frac{\kappa \Delta t}{16} \|\nabla T_h^{-1}\|^2) \\
(35) \quad & + \frac{\kappa^{-1} \Delta t}{2\beta} \|\gamma\|_{L^\infty(\mathbb{R}_+, W_h^*)}^2,
\end{aligned}$$

which is the result for long the time stability for the temperature. Letting $\mathbf{v}_h = \mathbf{u}_h^{n+1}$ in (26), and $q_h = p_h^{n+1}$ in (27), one obtains

$$\begin{aligned}
(36) \quad & \left(\frac{\frac{5}{3} \mathbf{u}_h^{n+1} - \frac{5}{2} \mathbf{u}_h^n + \mathbf{u}_h^{n-1} - \frac{1}{6} \mathbf{u}_h^{n-2}}{\Delta t}, \mathbf{u}_h^{n+1} \right) + \nu \|\nabla \mathbf{u}_h^{n+1}\|^2 \\
& = Ri(T^* \mathbf{e}_2, \mathbf{u}_h^{n+1}) + (\mathbf{f}^{n+1}, \mathbf{u}_h^{n+1}).
\end{aligned}$$

Repeating the arguments used for obtaining (19) yields

$$\begin{aligned}
(37) \quad & \|\mathcal{U}_{n+1}\|_G^2 - \|\mathcal{U}_n\|_G^2 + \frac{1}{12} \|\mathbf{u}_h^{n+1} - 3\mathbf{u}_h^n + 3\mathbf{u}_h^{n-1} - \mathbf{u}_h^{n-2}\|^2 \\
& + \frac{\nu \Delta t}{2} \|\nabla \mathbf{u}_h^{n+1}\|^2 \\
& \leq C_p^2 \nu^{-1} Ri^2 \Delta t \|T^*\|^2 \|\mathbf{e}_2\|^2 + \nu^{-1} \Delta t \|\mathbf{f}^{n+1}\|_{\mathbf{V}_h^*}.
\end{aligned}$$

Note that \mathbf{e}_2 is a unit vector, i.e., $\|\mathbf{e}_2\| = 1$ and using the definition of \mathcal{T}^* and (3), we get $\|\mathcal{T}^*\| \leq 7\|\mathcal{T}_n\| \leq 7\sqrt{C_u} \|\mathcal{T}_n\|_G$. Then, one has

$$\begin{aligned}
(38) \quad & \|\mathcal{U}_{n+1}\|_G^2 - \|\mathcal{U}_n\|_G^2 + \frac{1}{12} \|\mathbf{u}_h^{n+1} - 3\mathbf{u}_h^n + 3\mathbf{u}_h^{n-1} - \mathbf{u}_h^{n-2}\|^2 + \frac{\nu \Delta t}{2} \|\nabla \mathbf{u}_h^{n+1}\|^2 \\
& \leq 49C_u C_p^2 \nu^{-1} Ri^2 \Delta t \|\mathcal{T}_n\|_G^2 + \nu^{-1} \Delta t \|\mathbf{f}^{n+1}\|_{\mathbf{V}_h^*}.
\end{aligned}$$

Arguing as in (20), one gets the following estimation for (38)

$$\begin{aligned}
(39) \quad & (1 + \alpha) (\|\mathcal{U}_{n+1}\|_G^2 + \frac{\nu \Delta t}{4} \|\nabla \mathbf{u}_h^{n+1}\|^2 + \frac{\nu \Delta t}{16} \|\nabla \mathbf{u}_h^n\|^2) \\
& \leq (\|\mathcal{U}_n\|_G^2 + \frac{\nu \Delta t}{4} \|\nabla \mathbf{u}_h^n\|^2 + \frac{\nu \Delta t}{16} \|\nabla \mathbf{u}_h^{n-1}\|^2) \\
& + 49C_u C_p^2 \nu^{-1} Ri^2 \Delta t \|\mathcal{T}_n\|_G^2 + \nu^{-1} \Delta t \|\mathbf{f}^{n+1}\|_{\mathbf{V}_h^*}
\end{aligned}$$

where $\alpha = \min\{\frac{C_l \nu \Delta t}{16C_p^2}, \frac{3}{4}\}$. Putting n instead of $(n+1)$ in (35) and inserting it in (39) yields

$$\begin{aligned}
(40) \quad & (1 + \alpha) (\|\mathcal{U}_{n+1}\|_G^2 + \frac{\nu \Delta t}{4} \|\nabla \mathbf{u}_h^{n+1}\|^2 + \frac{\nu \Delta t}{16} \|\nabla \mathbf{u}_h^n\|^2) \\
& \leq (\|\mathcal{U}_n\|_G^2 + \frac{\nu \Delta t}{4} \|\nabla \mathbf{u}_h^n\|^2 + \frac{\nu \Delta t}{16} \|\nabla \mathbf{u}_h^{n-1}\|^2) \\
& + 49C_u C_p^2 \nu^{-1} Ri^2 \Delta t \left((1 + \beta)^{-n} (\|\mathcal{T}_0\|_G^2 + \frac{\kappa \Delta t}{4} \|\nabla T_h^0\|^2 \right. \\
& \left. + \frac{\kappa \Delta t}{16} \|\nabla T_h^{-1}\|^2) + \frac{\kappa^{-1} \Delta t}{2\beta} \|\gamma\|_{L^\infty(\mathbb{R}_+, W_h^*)}^2 \right) + \nu^{-1} \Delta t \|\mathbf{f}^{n+1}\|_{\mathbf{V}_h^*}.
\end{aligned}$$

Applying induction and adding (35) to (40) completes the proof of the theorem. \square

4.1. Numerical experiment for natural convection equations. In this subsection, we present the long time numerical simulation results of a coupled Navier-Stokes system given by the scheme (26)-(28). We consider natural convection equations in $\Omega = (0, 1)^2$ with a coarse mesh resolution of 16×16 . For this problem, we solve a buoyancy driven cavity test in which, upper and lower boundaries of the square domain are kept adiabatic and vertical boundaries are kept at different temperatures imposed as Dirichlet boundary conditions. The flow initiates naturally by density differences due to the temperature variations at opposing vertical boundaries along with the gravitational force. The domain presented in Figure 2 is used in the numerical test. Velocity boundary conditions are no-slip everywhere. We set the Richardson number, $Ri = 1$ and perform the computation in the time interval $[0, 150]$. The results for different viscosities and time step sizes are provided. We examine the time evolution of the computed solutions in discrete norms $\|\mathbf{u}_h^n\|$ and $\|T_h^n\|$.

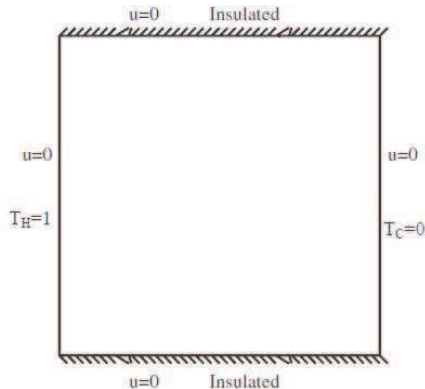


FIGURE 2. The computational domain for the natural convection test example.

A clear observation from Figure 3, both velocity and temperature solutions are globally in time bounded for varying viscosity instances. As we expect, due to the nature of these flows, narrow oscillation intervals could be observed for smaller ν values but still we can conclude that the solutions are all long time stable as theory predicts.

Similar to the Navier-Stokes case, we present the comparison table of CPU times in order to feel the computational advantage of the BLEBDF in Table 2. Since the degree of freedom of overall system has been increased in natural convection case, we observe more visible CPU time differences in our comparison with the classical BDF2 scheme. Also we have used a rather short time interval for this test case. One could conclude from this comparison that, using the BLEBDF scheme instead of BDF2 scheme will yield a computational time advantage when smaller time step sizes are used on longer time intervals.

5. Long time stability of double-diffusive convection with BLEBDF

Under the assumption of Boussinesq approximation, we consider a fluid flow in Ω with a polygonal boundary $\partial\Omega = \Gamma_T \cup \Gamma_B$ with $\Gamma_T \cap \Gamma_B = \emptyset$. The governing equations of double-diffusive convection known as also Darcy-Brinkman system are

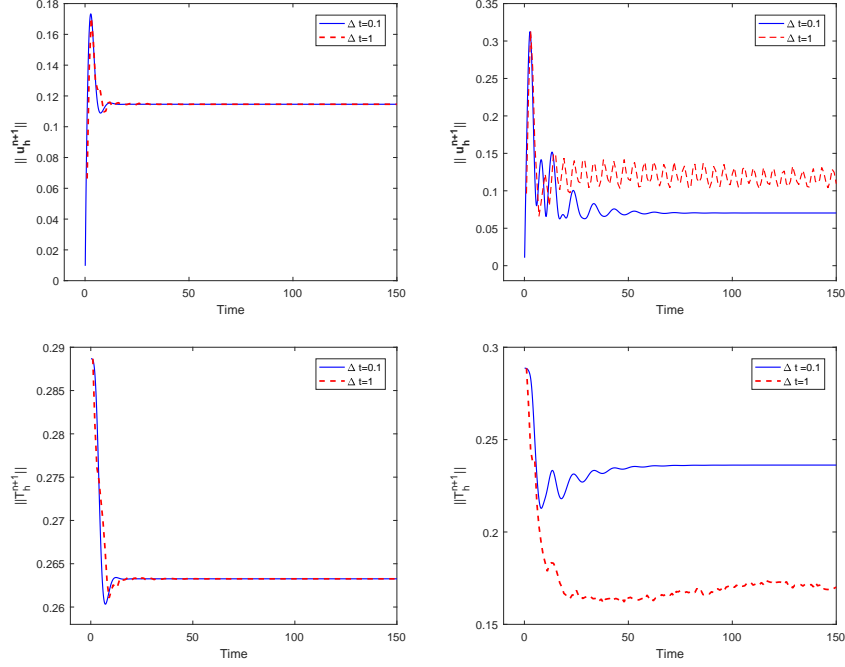


FIGURE 3. Evolution of the L^2 norm of the solution for varying viscosities. Velocity for $\nu = 0.01$, $\nu = 0.001$ (upper left to right) and temperature for $\nu = 0.01$, $\nu = 0.001$ (lower left to right).

TABLE 2. Comparison of the CPU-times (seconds) of classical BDF2 scheme and BLEBDF for natural convection with $\nu = 0.001$ on a time interval $[0, 10]$.

Δt	BDF2	BLEBDF
1	6.71	6.27
0.1	61.8	59
0.01	628	610

given by (see e.g. [7]),

$$\begin{aligned}
 \mathbf{u}_t - \nu \Delta \mathbf{u} + (\mathbf{u} \cdot \nabla) \mathbf{u} + Da^{-1} \mathbf{u} + \nabla p &= (\beta_T T + \beta_C C) \mathbf{g} + \mathbf{f} && \text{in } \Omega, \\
 \nabla \cdot \mathbf{u} &= 0 && \text{in } \Omega, \\
 T_t - \gamma \Delta T + \mathbf{u} \cdot \nabla T &= \kappa && \text{in } \Omega, \\
 C_t - D_c \Delta C + \mathbf{u} \cdot \nabla C &= \zeta && \text{in } \Omega, \\
 \mathbf{u}(0, \mathbf{x}) = \mathbf{u}_0, T(0, \mathbf{x}) = T_0, C(0, \mathbf{x}) &= C_0 && \text{in } \Omega, \\
 \mathbf{u} = \mathbf{0} \text{ on } \partial\Omega, T, C &= 0 && \text{on } \Gamma_T, \\
 \frac{\partial T}{\partial \mathbf{n}} = 0, \frac{\partial C}{\partial \mathbf{n}} &= 0 && \text{on } \Gamma_B.
 \end{aligned}
 \tag{41}$$

Besides the parameters defined earlier, C is the concentration, C_0 the initial fluid concentration and ζ the body force for concentration equation. We also have the Darcy number Da , the thermal conductivity κ , the mass diffusivity $D_c > 0$, \mathbf{g} the gravitational acceleration vector, the thermal and solutal expansion coefficients are β_T , β_C , respectively. The dimensionless parameters are the buoyancy ratio

$N = \frac{\beta_C \Delta C}{\beta_T \Delta T}$, the Schmidt number $Sc = \frac{\nu}{D_c}$, Prandtl number $Pr = \frac{\nu}{\gamma}$, the Darcy number $Da = \frac{K}{H^2}$, the Lewis number $Le = \frac{Sc}{Pr}$ and the thermal Rayleigh number $Ra = \frac{\mathbf{g} \beta_T \Delta T H^3}{\nu \gamma}$. Here the cavity height is H and permeability is K . ΔT and ΔC are the temperature and concentration differences, respectively.

The fully discrete approximation of (41) based on the BLEBDF scheme reads as; for each time level, we look for approximations $(\mathbf{u}_h^{n+1}, T_h^{n+1}, C_h^{n+1}) \in (\mathbf{X}_h, W_h, \Psi_h)$, satisfying

$$(42) \quad \begin{aligned} & \left(\frac{\frac{5}{3} \mathbf{u}_h^{n+1} - \frac{5}{2} \mathbf{u}_h^n + \mathbf{u}_h^{n-1} - \frac{1}{6} \mathbf{u}_h^{n-2}}{\Delta t}, \mathbf{v}_h \right) + \nu (\nabla \mathbf{u}_h^{n+1}, \nabla \mathbf{v}_h) \\ & + b_1(\mathbf{u}^*, \mathbf{u}_h^{n+1}, \mathbf{v}_h) + Da^{-1}(\mathbf{u}_h^{n+1}, \mathbf{v}_h) \\ & = \left((\beta_T T^* + \beta_C C^*) \mathbf{g}, \mathbf{v}_h \right) + (\mathbf{f}^{n+1}, \mathbf{v}_h), \end{aligned}$$

$$(43) \quad \begin{aligned} & \left(\frac{\frac{5}{3} T_h^{n+1} - \frac{5}{2} T_h^n + T_h^{n-1} - \frac{1}{6} T_h^{n-2}}{\Delta t}, S_h \right) + \kappa (\nabla T_h^{n+1}, \nabla S_h) \\ & + b_2(\mathbf{u}^*, T_h^{n+1}, S_h) = (\gamma^{n+1}, S_h), \end{aligned}$$

$$(44) \quad \begin{aligned} & \left(\frac{\frac{5}{3} C_h^{n+1} - \frac{5}{2} C_h^n + C_h^{n-1} - \frac{1}{6} C_h^{n-2}}{\Delta t}, \phi_h \right) + b_3(\mathbf{u}^*, C_h^{n+1}, \phi_h) \\ & + D_c (\nabla C_h^{n+1}, \nabla \phi_h) = (\zeta^{n+1}, \phi_h). \end{aligned}$$

for all $(\mathbf{v}_h^{n+1}, S_h^{n+1}, \phi_h^{n+1}) \in (\mathbf{X}_h, W_h, \Psi_h)$ where $\mathbf{u}^* = \mathbf{u}_h^{n+1} = 3\mathbf{u}_h^n - 3\mathbf{u}_h^{n-1} + \mathbf{u}_h^{n-2}$, $T^* = T_h^{n+1} = 3T_h^n - 3T_h^{n-1} + T_h^{n-2}$ and $C^* = C_h^{n+1} = 3C_h^n - 3C_h^{n-1} + C_h^{n-2}$

This section is devoted to prove the long time stability of the solutions of (42)-(44).

Theorem 5.1. *(Unconditional long time stability of double-diffusive convection in L^2) Assume $\mathbf{f} \in L^\infty(\mathbb{R}_+, \mathbf{V}_h^*)$, $\gamma \in L^\infty(\mathbb{R}_+, W_h^*)$ and $\zeta \in L^\infty(\mathbb{R}_+, \Psi_h^*)$, then the approximation (42)-(44) is long time stable in the following sense: for any $\Delta t > 0$,*

$$\begin{aligned} & \|\mathcal{U}_{n+1}\|_G^2 + \|\mathcal{T}_{n+1}\|_G^2 + \|\mathcal{C}_{n+1}\|_G^2 + \frac{\nu \Delta t}{4} \|\nabla \mathbf{u}_h^{n+1}\|^2 + \frac{\kappa \Delta t}{4} \|\nabla T_h^{n+1}\|^2 \\ & + \frac{D_c \Delta t}{4} \|\nabla C_h^{n+1}\|^2 + \frac{Da^{-1} \Delta t}{4} \|\mathbf{u}_h^{n+1}\|^2 \\ & \leq (1 + \alpha)^{-(n+1)} \left(\|\mathcal{U}_0\|_G^2 + \frac{\nu \Delta t}{4} \|\nabla \mathbf{u}_h^0\|^2 + \frac{\nu \Delta t}{16} \|\nabla \mathbf{u}_h^{-1}\|^2 + \frac{Da^{-1} \Delta t}{4} \|\mathbf{u}_h^0\|^2 \right. \\ & + \frac{Da^{-1} \Delta t}{16} \|\mathbf{u}_h^{-1}\|^2 \left. \right) + (K_{T,\alpha} + (1 + \beta)^{-1}) \left((1 + \beta)^{-n} (\|\mathcal{T}_0\|_G^2 + \frac{\kappa \Delta t}{4} \|\nabla T_h^0\|^2 \right. \\ & + \frac{\kappa \Delta t}{16} \|\nabla T_h^{-1}\|^2) \left. \right) + (K_{C,\alpha} + (1 + \delta)^{-1}) \left((1 + \delta)^{-n} (\|\mathcal{C}_0\|_G^2 + \frac{D_c \Delta t}{4} \|\nabla C_h^0\|^2 \right. \\ & + \frac{D_c \Delta t}{16} \|\nabla C_h^{-1}\|^2) \left. \right) + (K_{T,\alpha} + 1) \max\left\{ \frac{8C_p^2}{C_l \kappa^2}, \frac{2\kappa^{-1} \Delta t}{3} \right\} \|\gamma\|_{L^\infty(\mathbb{R}_+, W_h^*)}^2 \\ & + (K_{C,\alpha} + 1) \max\left\{ \frac{8C_p^2}{C_l D_c^2}, \frac{2D_c^{-1} \Delta t}{3} \right\} \|\zeta\|_{L^\infty(\mathbb{R}_+, \Psi_h^*)}^2 \end{aligned}$$

$$(45) \quad + \max\left\{\frac{8C_p^2}{C_l\nu(\nu + C_p^2 Da^{-1})}, \frac{2\nu^{-1}\Delta t}{3}\right\} \|\mathbf{f}\|_{L^\infty(\mathbb{R}_+, \mathbf{V}_h^*)}^2,$$

$$\text{where } K_{T,\alpha} = \frac{49C_u Da \Delta t \|\mathbf{g}\|_\infty^2 \beta_T^2}{16C_p^2}, \quad K_{C,\alpha} = \frac{49C_u Da \Delta t \|\mathbf{g}\|_\infty^2 \beta_C^2}{16C_p^2},$$

$$\mathcal{U}_0 = [\mathbf{u}_h^0 \quad \mathbf{u}_h^{-1} \quad \mathbf{u}_h^{-2}], \quad \mathcal{T}_0 = [T_h^0 \quad T_h^{-1} \quad T_h^{-2}], \quad \mathcal{C}_0 = [C_h^0 \quad C_h^{-1} \quad C_h^{-2}],$$

$$\alpha = \min\left\{\frac{C_l(\nu + C_p^2 Da^{-1})\Delta t}{16C_p^2}, \frac{3}{4}\right\}, \quad \beta = \min\left\{\frac{C_l \kappa \Delta t}{16C_p^2}, \frac{3}{4}\right\}, \quad \delta = \min\left\{\frac{C_l D_c \Delta t}{16C_p^2}, \frac{3}{4}\right\}.$$

Proof. Arguing in the same way as for (35), letting $S_h = T_h^{n+1}$ in (43) and $\phi_h = C_h^{n+1}$ in (44) gives

$$(46) \quad \begin{aligned} & \|\mathcal{T}_{n+1}\|_G^2 + \frac{\kappa \Delta t}{4} \|\nabla T_h^{n+1}\|^2 + \frac{\kappa \Delta t}{16} \|\nabla T_h^n\|^2 \\ & \leq (1 + \beta)^{-(n+1)} (\|\mathcal{T}_0\|_G^2 + \frac{\kappa \Delta t}{4} \|\nabla T_h^0\|^2 + \frac{\kappa \Delta t}{16} \|\nabla T_h^{-1}\|^2) \\ & \quad + \frac{\kappa^{-1} \Delta t}{2\beta} \|\gamma\|_{L^\infty(\mathbb{R}_+, W_h^*)}^2 \end{aligned}$$

for the temperature where $\beta = \min\left\{\frac{C_l \kappa \Delta t}{16C_p^2}, \frac{3}{4}\right\}$ and

$$(47) \quad \begin{aligned} & \|\mathcal{C}_{n+1}\|_G^2 + \frac{D_c \Delta t}{4} \|\nabla C_h^{n+1}\|^2 + \frac{D_c \Delta t}{16} \|\nabla C_h^n\|^2 \\ & \leq (1 + \delta)^{-(n+1)} (\|\mathcal{C}_0\|_G^2 + \frac{D_c \Delta t}{4} \|\nabla C_h^0\|^2 + \frac{D_c \Delta t}{16} \|\nabla C_h^{-1}\|^2) \\ & \quad + \frac{D_c^{-1} \Delta t}{2\delta} \|\zeta\|_{L^\infty(\mathbb{R}_+, \Psi_h^*)}^2 \end{aligned}$$

for the concentration where $\delta = \min\left\{\frac{C_l D_c \Delta t}{16C_p^2}, \frac{3}{4}\right\}$ and $\mathcal{C}_{n+1} = [C_h^{n+1} \quad C_h^n \quad C_h^{n-1}]^\top$

and $\mathcal{C}_n = [C_h^n \quad C_h^{n-1} \quad C_h^{n-2}]^\top$. Next, a bound for the velocity begins with letting $\mathbf{v}_h = \mathbf{u}_h^{n+1}$ in (42), utilizing the similar ideas, one finds

$$(48) \quad \begin{aligned} & \|\mathcal{U}_{n+1}\|_G^2 - \|\mathcal{U}_n\|_G^2 + \frac{1}{12} \|\mathbf{u}_h^{n+1} - 3\mathbf{u}_h^n + 3\mathbf{u}_h^{n-1} - \mathbf{u}_h^{n-2}\|^2 \\ & \quad + \frac{\nu \Delta t}{2} \|\nabla \mathbf{u}_h^{n+1}\|^2 + \frac{Da^{-1} \Delta t}{2} \|\mathbf{u}_h^{n+1}\|^2 \\ & \leq Da \Delta t \|\mathbf{g}\|_\infty^2 (\beta_T^2 \|T^*\|^2 + \beta_C^2 \|C^*\|^2) + \frac{\nu^{-1} \Delta t}{2} \|\mathbf{f}^{n+1}\|_{\mathbf{V}_h^*}^2. \end{aligned}$$

As for (39), adding $\frac{\nu \Delta t}{4} \|\nabla \mathbf{u}_h^n\|^2 + \frac{\nu \Delta t}{16} \|\nabla \mathbf{u}_h^{n-1}\|^2 + \frac{Da^{-1} \Delta t}{4} \|\mathbf{u}_h^n\|^2 + \frac{Da^{-1} \Delta t}{16} \|\mathbf{u}_h^{n-1}\|^2$ to the both sides and arguing exactly in the same way, (48) yields

$$(49) \quad \begin{aligned} & (1 + \alpha) (\|\mathcal{U}_{n+1}\|_G^2 + \frac{\nu \Delta t}{4} \|\nabla \mathbf{u}_h^{n+1}\|^2 + \frac{\nu \Delta t}{16} \|\nabla \mathbf{u}_h^n\|^2 \\ & \quad + \frac{Da^{-1} \Delta t}{4} \|\mathbf{u}_h^{n+1}\|^2 + \frac{Da^{-1} \Delta t}{16} \|\mathbf{u}_h^n\|^2) \\ & \leq (\|\mathcal{U}_n\|_G^2 + \frac{\nu \Delta t}{4} \|\nabla \mathbf{u}_h^n\|^2 + \frac{\nu \Delta t}{16} \|\nabla \mathbf{u}_h^{n-1}\|^2 + \frac{Da^{-1} \Delta t}{4} \|\mathbf{u}_h^n\|^2 \\ & \quad + \frac{Da^{-1} \Delta t}{16} \|\mathbf{u}_h^{n-1}\|^2) + Da \Delta t \|\mathbf{g}\|_\infty^2 (\beta_T^2 \|T^*\|^2 + \beta_C^2 \|C^*\|^2) + \frac{\nu^{-1} \Delta t}{2} \|\mathbf{f}^{n+1}\|_{\mathbf{V}_h^*}^2 \end{aligned}$$

where $\alpha = \min\left\{\frac{\Delta t C_l}{16} \left(\frac{\nu}{C_p^2} + Da^{-1}\right), \frac{3}{4}\right\}$.

Utilizing (3), and the definitions of \mathcal{T}^* , \mathcal{C}^* , we get $\|\mathcal{T}^*\| \leq 7\|\mathcal{T}_n\| \leq 7\sqrt{C_u}\|\mathcal{T}_n\|_G$ and $\|\mathcal{C}^*\| \leq 7\|\mathcal{C}_n\| \leq 7\sqrt{C_u}\|\mathcal{C}_n\|_G$. Putting n instead of $(n+1)$ in (46) and (47) and inserting them in (49) yields

$$\begin{aligned}
& (1 + \alpha)(\|\mathcal{U}_{n+1}\|_G^2 + \frac{\nu\Delta t}{4}\|\nabla\mathbf{u}_h^{n+1}\|^2 + \frac{\nu\Delta t}{16}\|\nabla\mathbf{u}_h^n\|^2 \\
& \quad + \frac{Da^{-1}\Delta t}{4}\|\mathbf{u}_h^{n+1}\|^2 + \frac{Da^{-1}\Delta t}{16}\|\mathbf{u}_h^n\|^2) \\
& \leq (\|\mathcal{U}_n\|_G^2 + \frac{\nu\Delta t}{4}\|\nabla\mathbf{u}_h^n\|^2 + \frac{\nu\Delta t}{16}\|\nabla\mathbf{u}_h^{n-1}\|^2 + \frac{Da^{-1}\Delta t}{4}\|\mathbf{u}_h^n\|^2 \\
& \quad + \frac{Da^{-1}\Delta t}{16}\|\mathbf{u}_h^{n-1}\|^2) + 49C_u Da\Delta t\|\mathbf{g}\|_\infty^2 \left(\beta_T^2 \left((1 + \beta)^{-n} (\|\mathcal{T}_0\|_G^2 \right. \right. \\
& \quad \left. \left. + \frac{\kappa\Delta t}{4}\|\nabla T_h^0\|^2 + \frac{\kappa\Delta t}{16}\|\nabla T_h^{-1}\|^2) + \frac{\kappa^{-1}\Delta t}{2\beta}\|\gamma\|_{L^\infty(\mathbb{R}_+, W_h^*)}^2 \right) \right) \\
& \quad + \beta_C^2 \left((1 + \delta)^{-n} (\|\mathcal{C}_0\|_G^2 + \frac{D_c\Delta t}{4}\|\nabla C_h^0\|^2 + \frac{D_c\Delta t}{16}\|\nabla C_h^{-1}\|^2) \right. \\
& \quad \left. + \frac{D_c^{-1}\Delta t}{2\delta}\|\zeta\|_{L^\infty(\mathbb{R}_+, \Psi_h^*)}^2 \right) \Big) + \frac{\nu^{-1}\Delta t}{2}\|\mathbf{f}^{n+1}\|_{\mathbf{V}_h^*}^2.
\end{aligned} \tag{50}$$

Applying induction and summing up (50) with (46) and (47) gives the stated result (45). \square

5.1. Numerical experiment for double-diffusive convection. Among all the multiphysics flow examples issued in this study, the most challenging kind of flow is the double-diffusive convection case due to the highly oscillatory nature of its solutions [7, 16, 17]. As the Rayleigh number increases, complex behavior of the solutions becomes more visible. However, we could still show the long time stability of the solutions of this system with the moderate Rayleigh number of 1000 in a cavity convection case with the problem parameters, $N = 0.8$, $Le = 2$, $Pr = 1$. We study in a rectangular domain $\Omega = (0, 1) \times (0, 2)$ with a coarse mesh resolution of 10×20 . We note that, in the test, the Darcy number Da is taken to be infinity for convenience.

Similar to the the previous test, vertical boundaries are kept at different temperature and concentration values imposed as Dirichlet boundary conditions whereas, the velocity boundary conditions are still no-slip all over the boundary. For a better understanding, we illustrate the details of the computational domain in Figure 4 as in previous case.

In Figure 5, the evolutions of the norms of each variable are illustrated. It can be observed that for larger Δt values, solutions are stable inside an interval due to the complex attitude of the solution as explained earlier. However, the unconditional stability property of the solutions have been presented through this example.

In Table 3, we present the CPU time comparison table for the test problem. The most visible CPU time differences are occurred in this case due to the increment in the degrees of freedom. As one more equation has been coupled to the system compared with the previous test case, we feel the superiority of the BLEBDF scheme when compared to the classical BDF2 scheme especially for smaller Δt . So the BLEBDF is clearly preferable when solving coupling systems with small time step sizes on longer time intervals.

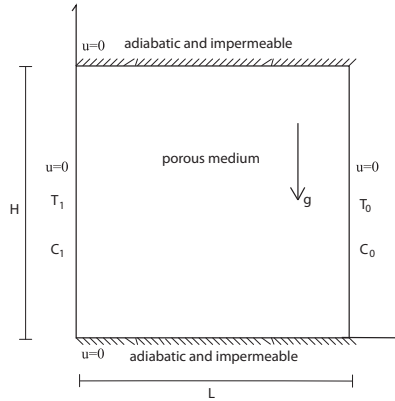


FIGURE 4. The computational domain for the double-diffusive convection test example.

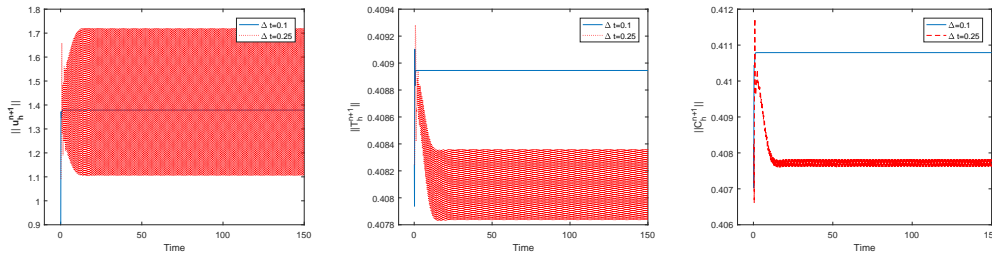


FIGURE 5. Evolution of the L^2 norm of the solution for $Ra = 10^3$, $Le = 2$, $Pr = 1$, $N = 0.8$.

TABLE 3. Comparison of the CPU-times (seconds) of classical BDF2 scheme and BLEBDF scheme for the double-diffusive convection test problem with $Ra = 10^3$ on a time interval $[0, 150]$.

Δt	BDF2	BLEBDF
1	9.41	9
0.1	92	88
0.01	1075	860

6. Conclusion

This study deals with the long time stability of multiphysics flow problems including the Navier-Stokes equations, natural convection and double-diffusive convection systems with BLEBDF temporal discretization along with the finite element method in spatial discretization. Unconditional stability of the schemes have been proven and theoretical results are supported with various numerical examples. Computed CPU times suggest that this method noticeably saves time compared

with the classical BDF2 scheme for small time step sizes. These numerical experiments establish the strong evidence of the long time stability results of multiphysics flows presented in this study.

References

- [1] R. A. Adams. Sobolev spaces. Academic Press, New York, 1975.
- [2] M. Akbas, S. Kaya and L. G. Rebholz. On the stability at all times of linearly extrapolated BDF2 timestepping for multiphysics incompressible flow problems. *Numer. Methods Partial Differ. Equ.*, 33(4):999–1017, 2017.
- [3] B. Ewald and F. Tone. Approximation of the long-term dynamics of the dynamical system generated by the two-dimensional thermohydraulics equations. *Int. J. Numer. Anal. Model.*, 10:509–535, 2013.
- [4] K. J. Galvin, A. Linke, L. G. Rebholz and N. E. Wilson. Stabilizing poor mass conservation in incompressible flow problems with large irrotational forcing and application to thermal convection. *Comput. Methods Appl. Mech. Engrg.* 237-240:166–176, 2012.
- [5] V. Girault and P. A. Raviart. Finite element approximation of the Navier-Stokes equations. *Lecture Notes in Math.*, Vol. 749, Springer-Verlag, Berlin, 1979.
- [6] S. Gottlieb, F. Tone, C. Wang, X. Wang, and D. Wirosoetisno. Long time stability of a classical efficient scheme for two-dimensional Navier-Stokes equations. *SIAM J. Numer. Anal.* 50:126–150, 2012.
- [7] B. Goyeau, J. P. Songbe, and D. Gobin. Numerical study of double-diffusive natural convection in a porous cavity using the Darcy-Brinkman formulation. *Int. J. Heat Mass Transfer*, 39:1363–1378, 1996.
- [8] E. Hairer and G. Wanner. Solving Ordinary Differential Equations II: Stiff and Differential Algebraic Problems, Second edition. Springer-Verlag, Berlin, 2002.
- [9] F. Hecht. New development in FreeFem++. *J. Numer. Math.* 20: 251–265, 2012.
- [10] T. Heister, M.A. Olshanskii and L.G. Rebholz. Unconditional long-time stability of a velocity-vorticity method for the 2D Navier-Stokes equations. *Numer. Math.* 135:143–167, 2017.
- [11] J. Heywood and R. Rannacher. Finite element approximation of the nonstationary Navier-Stokes problem. Part II: stability of solutions and error estimates uniform in time. *SIAM Journal on Numerical Analysis* 23(4):750–777, 1986.
- [12] J. Heywood and R. Rannacher. Finite element approximation of the nonstationary Navier-Stokes equations, IV: Error analysis for the second order time discretizations. *SIAM J. Numer. Anal.* 27:353–384, 1990.
- [13] W. Layton, H. Tran and C. Trenchea. Analysis of long time stability and errors of two partitioned methods for uncoupling evolutionary groundwater-surface water flows. *SIAM J. Numer. Anal.* 51:248–272, 2013.
- [14] W. Layton, H. Tran and C. Trenchea. Numerical analysis of two partitioned methods for uncoupling evolutionary MHD flows. *Numer. Methods Partial Differ. Equ.* 30:1083–1102, 2014.
- [15] M. Nyukhtikov, N. Smelova, B. E. Mitchell, and D. G. Holme. Optimized dual-time stepping technique for time-accurate Navier-Stokes calculations, *Unsteady Aerodynamics, Aeroacoustics and Aeroelasticity of Turbomachines*, Springer, Dordrecht, The Netherlands, 449–459, 2006.
- [16] Q. Qin, Z.A. Xia and Z.F. Tian. High accuracy numerical investigation of double-diffusive convection in a rectangular enclosure with horizontal temperature and concentration gradients. *Int. J. Heat Mass Transfer* 71:405–423, 2014.
- [17] S.S. Ravindran. An analysis of the blended three-step backward differentiation formula time-stepping scheme for the Navier-Stokes-type system related to Soret convection. *Numer. Funct. Anal. Optim.* 36:658–686, 2015.
- [18] J. Simo and F. Armero. Unconditional stability and long-term behavior of transient algorithms for the incompressible Navier-Stokes and Euler equations. *Comput. Methods Appl. Mech. Engrg.* 111(1):111–154, 1994.
- [19] F. Tone. On the long-time stability of the Crank-Nicholson scheme for the 2D Navier-Stokes equations. *Numer. Methods Partial Differ. Equ.* 23:5:1235–1248, 2007.
- [20] F. Tone. On the long-time H^2 -stability of the implicit Euler scheme for the 2D magnetohydrodynamics equations. *J. Sci. Comput.* 38:331–348, 2009.
- [21] F. Tone, X. Wang and D. Wirosoetisno. Long-time dynamics of 2d double-diffusive convection: analysis and/of numerics. *Numer. Math.* 130(3):541–566, 2015.

- [22] F. Tone and D. Wirosoetisno. On the long-time stability of the implicit Euler scheme for the two-dimensional Navier-Stokes equations. *SIAM J. Numer. Anal.* 44(1):29–40, 2006.
- [23] V. Vatsa, M. Carpenter and D. Lockard. Re-evaluation of an optimized second order backward difference (BDF2OPT) scheme for unsteady flow applications. *AIAA Paper*, 2010–122, 2010.
- [24] X. Wang. An efficient second order in time scheme for approximating long time statistical properties of the two dimensional Navier-Stokes equations. *Numer. Math.*, 121:753–779, 2012.

Department of Mathematics, Gazi University, 06550 Ankara, Turkey
E-mail: abayram@gazi.edu.tr

Department of Mathematics, Faculty of Science, Bartın University, 74110 Bartın, Turkey
E-mail: fguler@bartin.edu.tr

Department of Mathematics, Middle East Technical University, 06800 Ankara, Turkey
E-mail: smerdan@metu.edu.tr